THE EUROPEAN
PHYSICAL JOURNAL A

Regular Article – Experimental Physics

Measurement of Σ beam asymmetry in π^0 photoproduction off the neutron in the second and third resonances region[*]

R. Di Salvo[1], A. Fantini[1,10], G. Mandaglio[2,14], F. Mammoliti[2,11], O. Bartalini[3,10], V. Bellini[4,11], J.P. Bocquet[5], L. Casano[1], A. D'angelo[1,10], J.P. Didelez[6], D. Franco[1,10], G. Gervino[7,12], F. Ghio[8,13], G. Giardina[2,14], B. Girolami[8,13], A. Giusa[2,11], M. Guidal[6], E. Hourany[6†], R. Kunne[6], A. Lapik[9], P. Levi Sandri[3,a], A. Lleres[5], M. Manganaro[2,14], D. Moricciani[1], A.N. Mushkarenkov[9], V. Nedorezov[9], C. Randieri[3,11], D. Rebreyend[5], N. Rudnev[9], G. Russo[2,11], C. Schaerf[1,10], M.L. Sperduto[2,11], M.C. Sutera[2], A. Turinge[9], V. Vegna[1,10], A. Fix[15], S.S. Kamalov[16,17], and L. Tiator[16]

[1] INFN - Sezione di Roma "Tor Vergata", via della Ricerca Scientifica 1, I-00133 Roma, Italy
[2] INFN - Sezione di Catania, via Santa Sofia 64, I-95123 Catania, Italy
[3] INFN - Laboratori Nazionali di Frascati, via Enrico Fermi 40, I-00044 Frascati, Italy
[4] INFN - Laboratori Nazionali del Sud, via Santa Sofia 64, I-95123 Catania, Italy
[5] LPSC, Université Joseph Fourier Grenoble 1, CNRS/IN2P3, Institut National Polytechnique de Grenoble, 53 Avenue des Martyrs, 38026 Grenoble, France
[6] IPNO, Université de Paris-Sud 11, CNRS/IN2P3, 15 rue Georges Clémenceau, 91406 Orsay, France
[7] INFN - Sezione di Torino, via P. Giuria, I-10125 Torino, Italy
[8] INFN - Sezione di Roma, piazzale Aldo Moro 2, I-00185 Roma, Italy
[9] Institute for Nuclear Research, 117312 Moscow, Russia
[10] Dipartimento di Fisica, Università di Roma "Tor Vergata", via della Ricerca Scientifica 1, I-00133 Roma, Italy
[11] Dipartimento di Fisica e Astronomia Università di Catania, via Santa Sofia 64, I-95123 Catania, Italy
[12] Università di Torino, via P. Giuria, I-00125 Torino, Italy
[13] Istituto Superiore di Sanità, viale Regina Elena 299, I-00161 Roma, Italy
[14] Dipartimento di Fisica, Università di Messina, salita Sperone 31, I-98166 Messina, Italy
[15] Laboratory of Mathematical Physics, Tomsk Polytechnic University, 634050, Tomsk, Russia
[16] Institut für Kernphysik, Johannes Gutenberg-Universität Mainz, D-55099 Mainz, Germany
[17] Laboratory of Theoretical Physics, JINR Dubna, 141980 Moscow region, Russia

Abstract. The Σ beam asymmetry in the photoproduction of neutral pions from quasi-free nucleons in a deuteron target was measured for the first time between 0.60 and 1.50 GeV, with the GRAAL polarized and tagged photon beam. The asymmetry values from the quasi-free proton were found equal to the ones extracted from a pure proton target. The asymmetries from quasi-free proton and quasi-free neutron were found equal up to 0.82 GeV and substantially different at higher energies. The results are compared with recent partial-wave analyses.

PACS. 13.60.Le Meson production – 13.88.+e Polarization in interactions and scattering – 25.20.Lj Photoproduction reactions

1 Introduction

The availability over the last decade of high duty-cycle accelerators coupled with the use of large solid-angle detectors yielded a wealth of experimental information in the study of the photo- and electroproduction of mesons from the proton. The attempt is to extract, from photoproduction, the electromagnetic couplings and furthermore the hadronic properties of the excited nucleon states that cannot be accessed via pion scattering, either because the resonances largely overlap, or because of a weak coupling to the single pion-nucleon channel.

In hadronic reactions induced by real photons, the polarization degrees of freedom play a crucial role, and offer

---

a complementary approach to the baryon spectroscopy. Polarization observables arising from interference mechanisms, are highly sensitive to the details of the interaction revealing resonance properties that are difficult to extract from a cross-section measurement, where a single contribution often dominates [1–4].

The detailed description of the photon-nucleon interaction requires a complete data set containing, at least, eight independent observables: the cross-section, the three single polarization observables (beam, target and recoil nucleon) and four, appropriately chosen, double polarization observables [5]. The resonance properties can then be extracted from the photoproduction data via partial-wave analysis and multipole decomposition, in the framework of different approaches [3,6]. The comparison of the calculated observables with the experimental data becomes a strong constraint to the theoretical models [4,7], to determine the role and the properties of the resonance included.

The GRAAL Collaboration already provided a large amount of precise polarization and cross-section data for various meson photoproduction reactions on the proton. In particular, the Σ beam asymmetry and the differential cross-section were measured for π^0 photoproduction in the 0.55–1.50 GeV energy range [8], bringing essential constraints to the theoretical models and to partial-wave analysis, and allowing to determine, within the model of ref. [9] the spin of the new resonance $N(2070)$ D_{15} introduced in order to fit the large data set (see fig. 18 of ref. [8]). In order to obtain complementary information, and towards a full multipole analysis including the isospin structure, data on meson photoproduction from the neutron are of the utmost importance.

In sect. 2 we give a brief description of the experimental set-up. In sect. 3 the data analysis procedure is discussed, while in sect. 4 the Σ beam asymmetries on the proton bound in the deuterium nucleus are compared with those of the free proton; the asymmetries from the quasi-free neutron are presented and are compared with quasi-free proton results and with theoretical models. The effect of these data on the multipole expansion is discussed. The last section contains our conclusions.

2 Experimental set-up

The GRAAL experiment is based on the use of a tagged and polarized photon beam obtained through the Compton back-scattering of laser light off the 6.03 GeV electrons circulating in the ESRF storage ring. A full description of the beam characteristics can be found in ref. [8]. The coupling of the GRAAL beam with a large acceptance detector covering $0.95 \cdot 4\pi$ solid angle with cylindrical symmetry (Lagranγe) is the ideal tool in order to measure polarization degrees of freedom, in particular Σ beam asymmetries, with very small systematic errors. For the purposes of this paper it is important to remember that the detector is substantially divided into two parts:

1) a central part based on the BGO *Rugby Ball* calorimeter that covers laboratory angles $25° < \theta_{lab} < 155°$.

The calorimeter, coupled to a $\Delta E/\Delta x$ segmented scintillation counter (called *Barrel*) for particle identification, has an excellent energy resolution for photons [10] and a high detection efficiency ($> 40\%$ depending on the energy threshold) for neutrons [11];

2) a forward part ($\theta_{lab} < 25°$) equipped with two plane wire chambers, two scintillator walls and a *Forward Shower* detector having a good neutron detection efficiency ($\sim 22\%$) with momentum determination via time-of-flight (T.O.F.) measurement (~ 750 ps resolution for neutrons) [12].

The GRAAL experiment took data with a 6 cm length deuterium target in six different periods from June 1999 until December 2005. Both the 514 nm green line (giving rise to a 0.55–1.10 GeV tagged photon beam) and the 333–368 nm UV line (0.80–1.50 GeV tagged photons) from the Argon laser were used, with typical intensities of $\sim 10^6\gamma$/s. Data taking was triggered by the coincidence between a tagging signal (which determines the incident photon energy with 0.016 GeV FWHM resolution) and the total energy measured by the *Rugby Ball*, the latter being required to be greater than 0.18 GeV. This condition gave rise to a data acquisition rate ~ 100 events/s and allowed to record neutral pion photoproduction events both from quasi-free neutrons and quasi-free protons. The beam polarization can easily be changed by rotating the laser polarization. During data taking the polarization was moved from vertical (V) to horizontal (H) approximately every 20 minutes, defining two orthogonal polarization states. About 10% of the beam time was devoted to collect data with the unpolarized beam (electron Bremsstrahlung on the residual vacuum of the synchrotron doughnut).

3 Data analysis

Data on the neutral pion photoproduction from quasi-free protons and from quasi-free neutrons were simultaneously recorded and analysed in a similar way: two neutral signals in the BGO *Rugby Ball* were required to produce the π^0 invariant mass in the range 0.09–0.20 GeV/c^2 (initial preliminary selection see fig. 1).

Together with the two photons in the BGO, a proton or a neutron signal was required, either in the forward direction or in the BGO *Rugby Ball*. At forward angles, the proton was identified via ΔE *vs.* T.O.F. (both measured in the two scintillator wall) while a T.O.F. greater than 13.5 ns (measured in the *Forward Shower*) with no associated track in the other detectors was used to select the neutron. In the central region, the proton was identified from the E *vs.* ΔE (measured in the *Rugby Ball* and in the *Barrel*, respectively) whereas a low crystal multiplicity (less than five) was the selection criterion for the candidate neutron. To select quasi-free kinematics (participant-spectator approach), events with any additional signal(s) were rejected.

These events were then required to fulfill the two-body kinematics of the $\pi^0 N$ reaction, where N is the participating nucleon. Bidimensional cuts were applied on the following quantities:
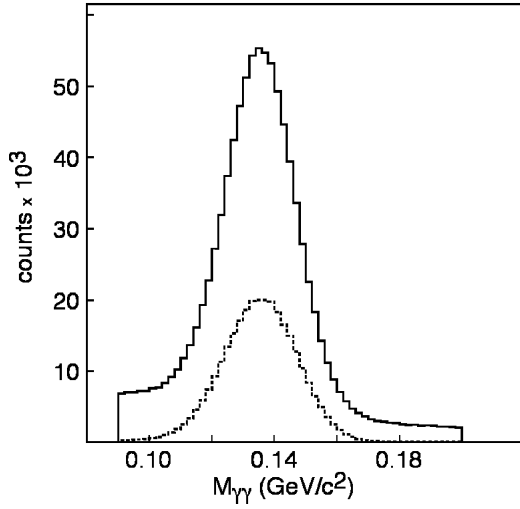
Fig. 1. Invariant mass of the two photons from π^0 decay before (full line) and after (dashed line) the kinematical cuts, when the neutron is detected in the forward direction. The obtained resolution is typical of the *Rugby Ball* calorimeter.
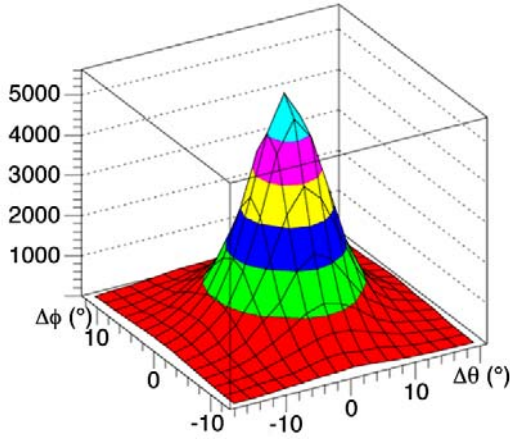

Fig. 2. (Colour on-line) The $\Delta\theta$ *vs.* $\Delta\phi$ distribution (see text for definitions of $\Delta\theta$ and $\Delta\phi$).

– $\Delta\theta$ *vs.* $\Delta\phi$, where $\Delta\theta = \theta_N - \theta_M$ is the polar angle difference between the measured and the theoretical angle required to fulfill the two-body kinematics calculated from E_γ, the measured energy $E_m^{\pi^0}$ and the π^0 production angle θ^{π^0}. $\Delta\phi$ is the difference $(-180°)$ of the measured azimuthal angles of π^0 and N;

– the ratio $E_c^{\pi^0}/E_m^{\pi^0}$ *vs.* M_x, where $E_c^{\pi^0}$ is the π^0 energy calculated from the π^0 and N measured angles, and M_x is the missing mass calculated from E_γ and $E_m^{\pi^0}$.

In fig. 2 an example for a single E_γ energy bin of $\Delta\theta$ *vs.* $\Delta\phi$ distribution is shown, while the $E_c^{\pi^0}/E_m^{\pi^0}$ *vs.* M_x distribution is displayed in fig. 3.

These two distributions were fitted with bidimensional Gaussian functions: the mean values μ_1, μ_2 and the standard deviations σ_1 and σ_2 of the generic variables v_1 and v_2 were thus obtained. If the two Gaussians are
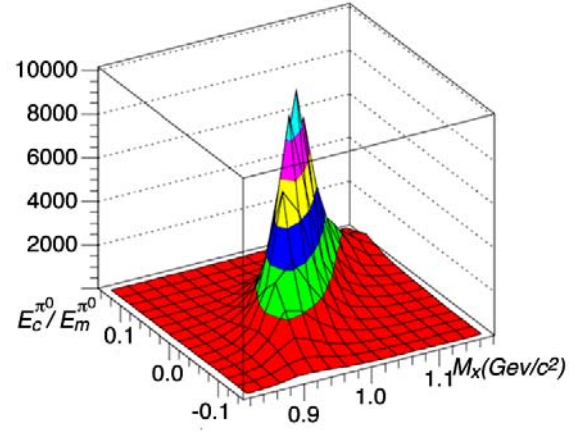

Fig. 3. (Colour on-line) The $E_c^{\pi^0}/E_m^{\pi^0}$ *vs.* M_x distribution (see text for definitions of $E_c^{\pi^0}$, $E_m^{\pi^0}$ and M_x).

uncorrelated the cut applied to v_1 and v_2 is

$$\frac{(v_1 - \mu_1)^2}{\sigma_1^2} + \frac{(v_2 - \mu_2)^2}{\sigma_2^2} < \sigma^2.$$

If the two variables are correlated, the correlation parameter C is extracted and the cut is defined as

$$\frac{(v_1 - \mu_1)^2}{\sigma_1^2} + \frac{(v_2 - \mu_2)^2}{\sigma_2^2} - 2C\frac{(v_1 - \mu_1)(v_2 - \mu_2)}{\sigma_1\sigma_2} < \sigma^2.$$

In the event selection a value $\sigma = 3$ was used and was determined by optimizing the signal/background ratio in a full Monte Carlo simulation including all competing channels, and based on the GEANT3 [13] package and a realistic event generator [14].

Since the backgrounds and the detector resolutions are a function of the energy of the incoming photon, the cuts are extracted and applied as a function of the energy bins. Once the events are selected, the beam asymmetry $\Sigma(E_\gamma, \theta_{cm})$ is extracted from the ratio

$$\frac{N_V/k_V}{N_V/k_V + N_H/k_H} = \frac{1}{2}(1 + P\Sigma\cos(2\phi)),$$

where N_H, N_V are the yields obtained with the two beam polarization states (horizontal and vertical), k_H, k_V are the corresponding beam intensities, $P(E_\gamma)$ is the degree of linear polarization of the beam at a given energy, $\Sigma(E_\gamma, \theta_{cm})$ is the asymmetry as a function of the incoming photon energy and of the polar angle of π^0 in the center-of-mass system, and ϕ is the π^0 azimuthal angle. For each bin of energy and θ_{cm}, the resulting ϕ distribution was fitted and the asymmetry $\Sigma(E_\gamma, \theta_{cm})$ extracted. A great care was used to determine θ_{cm}. The Fermi motion of the nucleon in the deuteron target is not negligible and the composition of the Fermi momentum with the momentum of the incident photon causes a rotation of the Lorentz boost axis off the direction of the beam. The evaluation of the Fermi momentum $\boldsymbol{p}_F$ from the momentum balance of the two-body kinematics

$$\boldsymbol{p}_F = \boldsymbol{p}_{\pi^0} + \boldsymbol{p}_N - \boldsymbol{p}_\gamma$$
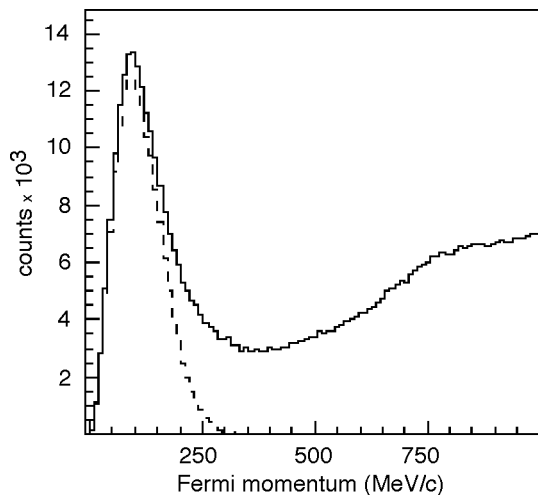
Fig. 4. The calculated neutron Fermi momentum distribution before (full line) and after (dashed line) the kinematical cuts.

is affected in particular by the imprecise knowledge of the momentum of the nucleon. The π^0 energy and π^0 and the nucleon emission angles are the more suitable information to use. Assuming a small Fermi energy (few MeV) for the nucleon in the deuteron, one can write

$$E_N^{extr} = E_\gamma + M_N - E_{\pi^0},$$
$$p_N^{extr} = \sqrt{(E_N^{extr})^2 - M_N^2},$$

where E_N^{extr} and p_N^{extr} are the extracted energy and momentum of the outgoing nucleon. The extracted momentum is then combined with the measured outgoing nucleon angles to determine the three Cartesian components. The Fermi momentum is then calculated as follows:

$$\boldsymbol{p}_F = \boldsymbol{p}_{\pi^0} + \boldsymbol{p}_N^{extr} - \boldsymbol{p}_\gamma.$$

At this point the θ_{cm} can be recalculated and the value obtained takes into account for the Fermi motion. In fig. 4, we show the Fermi momentum distribution before and after the bidimensional cuts are applied.

Data collected with the green laser line and with the UV laser line were analyzed separately and found compatible (at the level of 2 standard deviations at worst) in the overlap region, where a weighted average of Σ was performed. At the end of the event selection process, approximately $2.1 \cdot 10^6$ quasi-free neutron events and $6.9 \cdot 10^6$ quasi-free proton events were available for the extraction of the beam asymmetry $\Sigma(E_\gamma, \theta_{cm})$, and were grouped in 27 energy bins and 8 angular bins.

The main sources of systematic uncertainties affecting the cross-section measurement (total photon flux, solid-angle determination and deuterium density) cancel out when the Σ beam asymmetry is calculated. The only relevant contributions are related to the beam polarization and the hadronic background (misidentified reaction channels). They were estimated to give rise, added in quadrature, to a 3% total systematic uncertainty.

4 Results

4.1 Quasi-free proton

At the first step, the Σ beam asymmetry for the reaction $\gamma + p \rightarrow p + \pi^0$ for the quasi-free proton was derived and compared with the existing data collected at GRAAL on a pure proton target [8]. The same energy binning was used in order to achieve the best comparison of the two independent data sets. The results are displayed in fig. 5. We can see that there is an overall good agreement between the two independent data sets: the behavior of the asymmetry as a function of the center-of-mass angle of the neutral pion is the same for the free proton and for the quasi-free proton. There are only small differences at some energies, that can be ascribed to a smearing of the asymmetry value due to the Fermi motion. A similar effect was observed recently also in the beam asymmetry for η photoproduction [15]. Since the bound proton, adequately treated in the quasi-free kinematical regime, behaves similarly to the free proton when the beam asymmetry is measured, we are confident that the measured beam asymmetries for the π^0 photoproduction on the quasi-free neutron are very similar to the same observable measured on a free neutron if a free-neutron target were to exist.

4.2 Quasi-free neutron

The values of the Σ beam asymmetry for the quasi-free neutron are shown in fig. 6, where they are compared with the predictions of the MAID2007 [16] (dashed lines) and with the results of the modified MAID2007 version (solid lines). The last one includes in the fit the results of our measurement. The comparison with predictions of different models [17] is not shown since they are similar to MAID2007.

MAID2007 is a unitary isobar model which describes pion photoproduction in terms of background processes as Born terms and vector meson exchanges and nucleon resonance excitations.

The background processes are well determined and the couplings are fixed to the large database of pion photoproduction from protons. This is strictly valid only for multipoles with isospin 3/2. However, the multipoles with isospin 1/2 have independent contributions in the proton and neutron channels. The last one can only be obtained from data on pion photoproduction reactions from neutrons, included in the modified version of MAID2007.

As we can see from fig. 6, the main effects are at backward angles and above $0.9\,\mathrm{GeV}$ of the incident photon energy. The values of the asymmetry are positive at all energies and angles, in contrast with the results obtained for the free proton where a change in sign of the asymmetry occurs around $\theta_{cm}^{\pi^0} \approx 90°$ and for photon energies between 0.95 and $1.35\,\mathrm{GeV}$. The new version of the fit describes much better the behavior of the asymmetry: the negative values predicted by the MAID2007 version are absent from the modified MAID2007 result, and the overall behavior is reproduced.
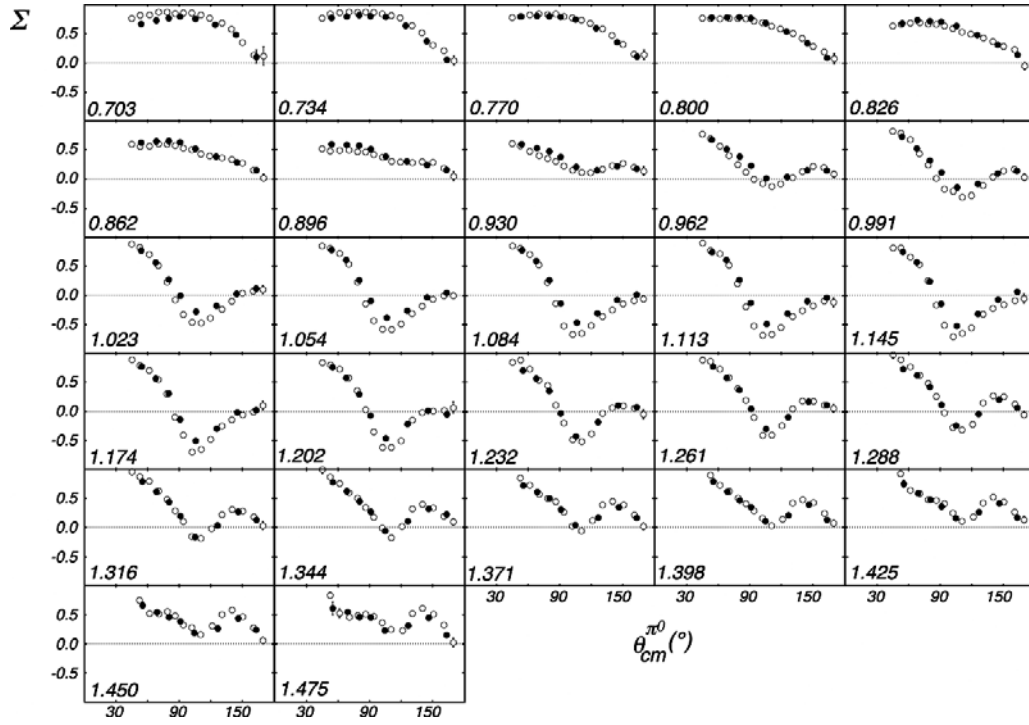
Fig. 5. The Σ beam asymmetry for the reaction $\gamma + p \to p + \pi^0$. Open dots refers to the GRAAL results on free proton [8]. Full dots are the result of this work for proton bound in the deuteron target in the quasi-free kinematic. Only the statistical uncertainty is shown.
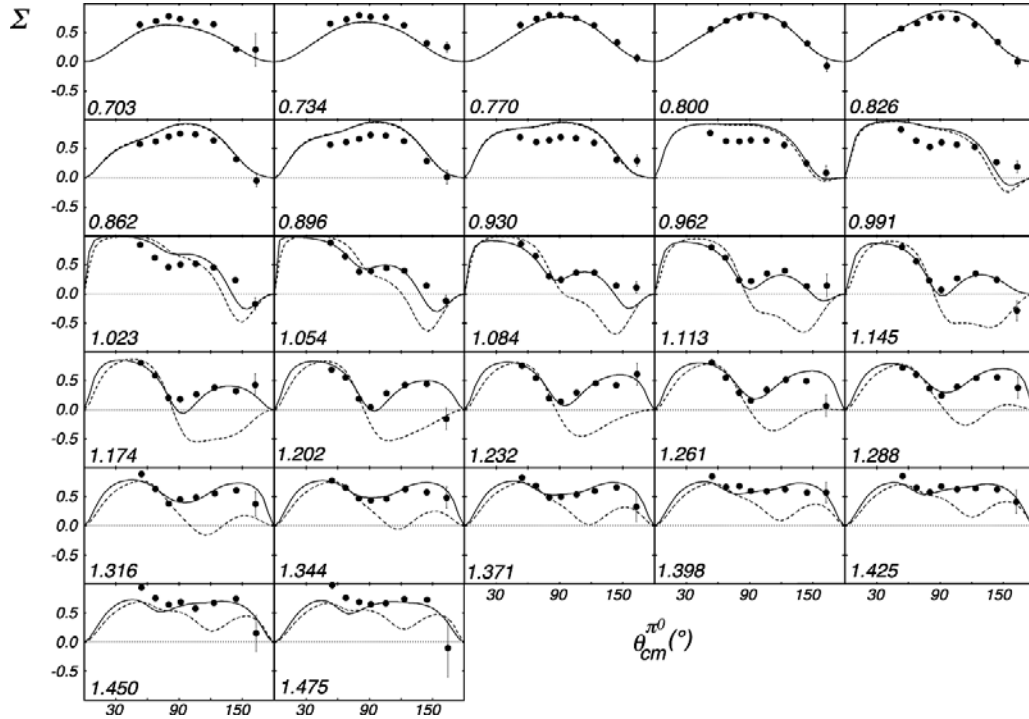

Fig. 6. The Σ beam asymmetry for the reaction $\gamma + n \to n + \pi^0$ compared with the predictions of MAID2007 (dashed line) and modified MAID2007 (full line). Where not visible, errors bars lie within the data point spots. Only the statistical uncertainty is shown.
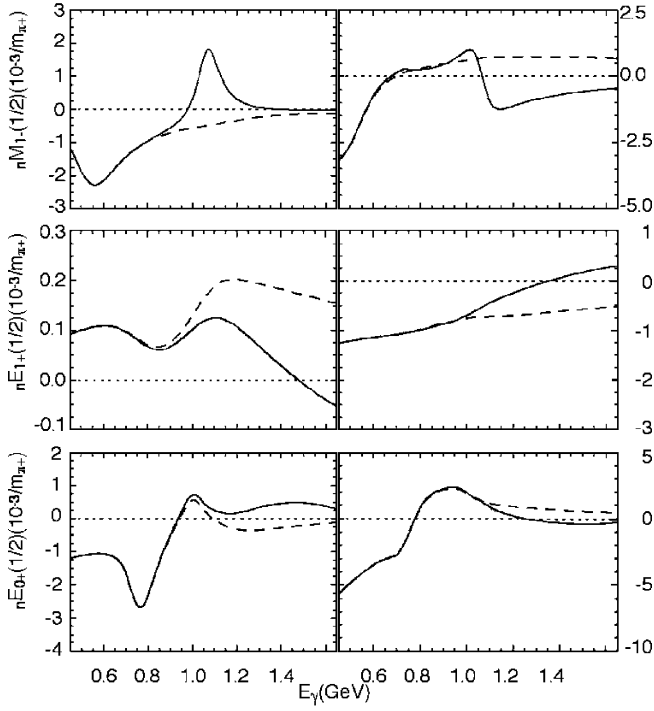
Fig. 7. MAID2007 [16] (dashed lines) and modified MAID2007 (solid lines) global solutions. Left side: imaginary part; right side: real part. Upper part of the figure: $_nM_{1-}^{1/2}$ multipole, central part: $_nE_{1+}^{1/2}$ multipole, lower part: $_nE_{0+}^{1/2}$ multipole (see text).

Fig. 8. Σ beam asymmetry for the π^0 photoproduction on the quasi-free proton (full dots) and quasi-free neutron (open dots) as a function of the photon energy at fixed π^0 center-of-mass angle, compared to the results of partial-wave analysis from modified MAID2007 (full line: proton, dashed line: neutron). Where not visible, errors bars lie within the data point spots.

In terms of multipoles, the impact of our new data is clearly visible in fig. 7, where the modified MAID2007 solution is compared with the previous solution. The effect is particularly striking for the $_nM_{1-}^{1/2}$ multipole (upper plot of fig. 7): here is also the contribution of a second P_{11}-resonance with $M_R = 1.70 \, \text{GeV}$, $\Gamma_{tot} = 0.07 \, \text{GeV}$, single-pion branching ratio $\beta_\pi = 0.1$ and helicity amplitude $A_{1/2} = -0.076 \, \text{GeV}^{-1/2}$. Note that the indication of the existence of a state at $W \approx 1.70 \, \text{GeV}$ was also found in the reaction $\gamma + p \to p + \pi^0$ (see fig. 15 in ref. [16]) as well as in η photoproduction on the neutron [18,19].

The effect of including our data in the fit is also visible in the $_nE_{1+}^{1/2}$ multipole (middle plot of fig. 7). To have a good description of our data, the photo-couplings for the $P_{13}(1720)$-resonance were modified to be $A_{1/2}^n = -0.003 \, \text{GeV}^{-1/2}$ and $A_{3/2}^n = -0.023 \, \text{GeV}^{-1/2}$ while the original MAID2007 fit assumed $A_{3/2}^n = -0.031 \, \text{GeV}^{-1/2}$.

Finally, for $E_\gamma > 1 \, \text{GeV}$, the beam asymmetry is also sensitive to the background contributions from the $_nE_{0+}^{1/2}$ and $_nE_{1+}^{1/2}$ multipoles, which were also changed in the modified MAID2007 solution.

In fig. 8, the beam asymmetry for both quasi-free proton and quasi-free neutron are compared, together with the modified MAID2007 results. Proton and neutron asymmetries are very similar at small angles and low energies, while they differ significantly at large angles.
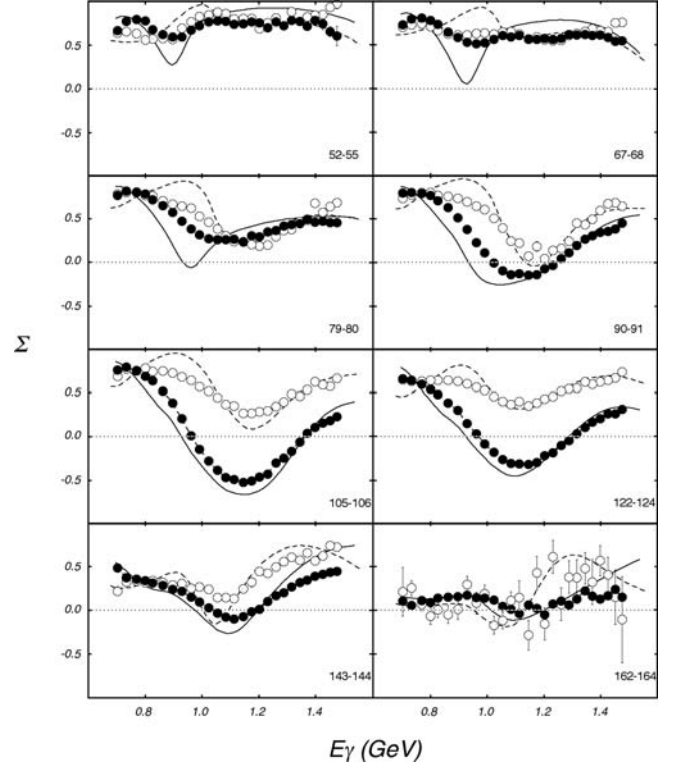
A big discrepancy with the fit results is present around $E_\gamma = 0.9 \, \text{GeV}$, corresponding to a total energy in the center-of-mass system of $\approx 1.7 \, \text{GeV}$ where the proton value is underestimated while the neutron value is over-predicted. The solution to this problem deserves further theoretical studies. From the experimental point of view, the complete determination of the isospin dependence in the beam asymmetry still requires the measurement of Σ in the $\pi^- p$ photoproduction off the neutron (i.e. $\gamma + n \to p + \pi^-$). The analysis of this reaction channel is underway at GRAAL [20] and the results will soon be available for theoretical interpretation and for partial-wave analysis.

5 Conclusions

The Σ beam asymmetry in the π^0 photoproduction off the nucleon bound in deuteron in the quasi-free kinematical regime was measured between 0.7 and 1.5 GeV photon energy, covering the second and the third nucleon resonance region. The results for the proton and for the quasi-free proton were found to be very similar, justifying a posteriori the participant-spectator approach. In the case of the quasi-free neutron, the asymmetry was found to be positive at all energies and center-of-mass angles. A modified

version of the MAID2007 model was able to reproduce the data when a second P_{11}-resonance with $M_R = 1.7\,\text{GeV}$ and $\Gamma_{tot} = 0.07\,\text{GeV}$ was added. Its effect is particularly visible in the $_nM_{1-}^{1/2}$ multipole. Further theoretical investigations are required to fully clarify the contributions to the transition amplitude in this energy region, and particularly around $1\,\text{GeV}$ of the incident photon energy.

References

1. M. Benmerrouche, N.C. Mukhopadhyay, J.F. Zhang, Phys. Rev. D **51**, 3237 (1995).
2. B. Saghai, F. Tabakin, Phys. Rev. C **55**, 917 (1997).
3. D. Drechsel, O. Hanstein, S.S. Kamalov, L. Tiator, Nucl. Phys. A **645**, 145 (1999).
4. T. Feuster, U. Mosel, Phys. Rev. C **59**, 460 (1999).
5. W.-T. Chiang, F. Tabakin, Phys. Rev. C **55**, 2034 (1997).
6. R.A. Arndt, I.I. Strakowsky, R.L. Workman, Phys. Rev. C **53**, 430 (1996).
7. B. Saghai, Z. Li, Eur. Phys. J. A **11**, 217 (2001).
8. O. Bartalini *et al.*, Eur. Phys. J. A **26**, 399 (2005).
9. A.V. Anisovich *et al.*, Eur. Phys. J. A **25**, 427 (2005).
10. P. Levi Sandri *et al.*, Nucl. Instrum. Methods A **370**, 396 (1996).
11. O. Bartalini *et al.*, Nucl. Instrum. Methods A **562**, 85 (2006).
12. V. Kuznetsov *et al.*, Nucl. Instrum. Methods A **487**, 396 (2002).
13. `http://wwwasd.web.cern.ch/wwwasd/geant/`.
14. P. Corvisiero *et al.*, Nucl. Instrum. Methods A **346**, 441 (1994).
15. A. Fantini *et al.*, Phys. Rev. C **78**, 015203 (2008).
16. D. Drechsel, S.S. Kamalov, L. Tiator, Eur. Phys. J. A **34**, 69 (2007); `http://www.kph.uni-mainz.de/MAID/`.
17. R.A. Arndt, I.I. Strakovsky, R.L. Workman, Int. J. Mod. Phys. A **18**, 449 (2003); `http://gwdac.phys.gwu.edu/`.
18. V. Kuznetsov *et al.*, Phys. Lett. B **647**, 23 (2007).
19. I. Jaegle *et al.*, Phys. Rev. Lett. **100**, 252002 (2008).
20. The GRAAL Collaboration, in preparation.